Scientific
Research

Sliding Mode Control with Auto-Tuning Law for Maglev System

Lingling Zhang[1], Zhizhou Zhang[2]*, Zhiqiang Long[2], Aming Hao[2]
[1]*College of Mathematics and Econometrics, Hunan University, Changsha, China*
[2]*College of Mechatronics Engineering and Automation, National University of Defense Technology, Changsha, China*
E-mail: *zzz*336@126.*com*

Abstract

This paper presents a control strategy for maglev system based on the sliding mode controller with auto-tuning law. The designed adaptive controller will replace the conventional sliding mode control (SMC) to eliminate the chattering resulting from the SMC. The stability of maglev system is ensured based on the Lyapunov theory. Simulation results verify the effectiveness of the proposed method. In addition, the advantages of the proposed controller are indicated in comparison with a traditional sliding mode controller.

1. Introduction

Maglev (Magnetic Levitation) train is a late-model railway vehicle with many good performances such as high speed, comfort, low environmental pollution, low energy consumption and so on. Lots of countries have started up the engineering study of maglev train [1,2].

The dynamic response of vehicle/guideway system affects the running safety, ride comfort and system costs heavily, which are crucial factors for maglev train commercial application [3,4]. Due to open-loop instability and inherent nonlinearities associated with a voltage-controlled magnetic levitation system, a feedback control is necessary to achieve a stable operation. Recently, quite a few control strategies have been developed and applied widely in the industrial field of maglev technology, such as bang-bang control [5], adaptive non-smooth control [6], hybrid control [7] and H_∞ control method [8], etc.

Sliding mode control is a powerful robust approach for controlling the nonlinear dynamic systems [9]. The advantage of sliding mode control is robustness against parameter matched uncertainties and external disturbance and so on. In general, vehicle-guide vibration of maglev system is easily subjected to external disturbance. Even though the approach of sliding mode control is one of potential control candidates for maglev system, it has some limitations such as discontinuous control law and chattering action, which lead to the appearance of input chattering, the high-frequency plant dynamics and unforeseen instability in real application. In order to alleviate the high-frequency chattering, control researchers have proposed many strategies, such as the boundary layer technique [10,11] and parameter identification mechanism with self-tuning [12,13]. In [14–16], using a modified hyperbolic tangent function as the activation function, the laws for tuning boundary layer thickness and control gain were proposed.

In this paper, the sliding mode control technique with auto-tuning law is applied to a voltage-controlled magnetic levitation system. The task of the control system is to dynamically regulate control voltage which drives the magnet to adjust the magnetic force to maintain a desired gap. Firstly, to simplify the mathematical model of maglev system, we discuss a 4-D maglev system via alternating physical variables of maglev system. In the following, with regard to this maglev system, four error variables are chosen to define the switching surface, and then a traditional sliding mode controller is designed accordingly [17]. In order to eliminate high-frequency control and chattering around the sliding surface, an auto-tuning neuron is introduced as an adaptive controller to guarantee the convergence of all states for maglev system. Simulations results show the control performance of our proposed method.

The paper is organized as follows: In Section 2, we give a mathematical model of maglev system, and then choose four error variables to determine the sliding surface. In Section 3, we design a general sliding mode controller and a systematic sliding mode controller with self-tuning law respectively. Simulation results will be given to validate the effectiveness of our proposed controller in Section 4. Conclusions are drawn in Section 5.

2. Sliding Surface Design of the Maglev System

The maglev system is a complicated system with machinery, controlling and electromagnetic elements integrated together. Figure 1 shows its working elements.

According to [3], m m denotes the weight of the electromagnet; and z represents the absolute displacement of the electromagnet in the vertical. R is the resistance of the electromagnet. I and $V(t)$ are current and voltage of the electromagnet winding, respectively. The control current I is driven by control voltage $V(t)$ to maintain the air gap z at its nominal value. Define $y = [y_1, y_2, y_3]^T = [z, \dot{z}, I]^T$, then dynamical and electromagnetic equations of the system are given as

$$\dot{y}_1 = y_2,$$
$$\dot{y}_2 = g - \frac{k}{m}\frac{y_3^2}{y_1^2}, \qquad (1)$$
$$\dot{y}_3 = \frac{y_2 y_3}{y_1} - \frac{R y_1 y_3}{2k} + \frac{y_1}{2k}V.$$

where $k = \frac{1}{4}\mu_0 N^2 S_0$, μ_0 is the magnetic permeability in vacuum, N is the number of turns of coil, and S_0 is the effective pole area of electromagnet.

Note that this electromagnetic suspension system is unstable without control voltage V. In closed-loop system, gap sensor measures the relative interval between electromagnet and guideway while accelerometer measures the absolute kinetic acceleration of the electromagnet. Based on feedback signals from sensors, the controller can generate certain control voltage according to control algorithm. With the calculated control voltage, the electromagnet can produce suitable electromagnetic force to keep itself suspending under the guideway stably.

In order to simplify the original nonlinear system (1), we choose the variable

$$X^* = [x_1^*, x_2^*, x_3^*, x_4^*]^T = [z, \dot{z}, I/Z, (I/Z)']^T = [y_1, y_2, y_3/y_1, (y_3/y_1)']^T,$$

x_3^* represents electromotive force of the electromagnet winding which has actual physical meanings. Then the model (1) can be transformed as following:
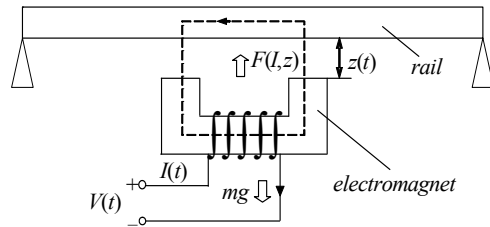

Figure 1. Structure of the maglev system.

$$\dot{x}_1^* = x_2^*,$$
$$\dot{x}_2^* = g - \frac{k x_3^{*2}}{m},$$
$$\dot{x}_3^* = x_4^*, \qquad (2)$$
$$\dot{x}_4^* = -\frac{R}{2k}(x_1^* x_4^* + x_2^* x_3^*) + \frac{1}{2k}V',$$

where $V'(x_1^*, x_2^*, x_3^*, x_4^*)$ is the derivatives of $V(x_1^*, x_2^*, x_3^*, x_4^*)$. And the values of the state variables at the balance point are $X_0^* = [z_0, 0, \sqrt{mg/k}, 0]$, where z_0 is a nominal value of the air gap z.

Moving the equilibrium to the origin, letting $X = [x_1, x_2, x_3, x_4]^T$, where $x_1 = x_1^* - z_0$, $x_2 = x_2^*$, $x_3 = x_3^* - \sqrt{mg/k}$, $x_4 = x_4^*$, (2) becomes

$$\dot{x}_1 = x_2,$$
$$\dot{x}_2 = -\frac{k x_3^2}{m} - 2\sqrt{kg/m}\, x_3,$$
$$\dot{x}_3^* = x_4^*, \qquad (3)$$
$$\dot{x}_4^* = -\frac{R}{2k}\left((x_1 + z_0)x_4 + (x_3 + \sqrt{mg/k})x_2\right) + \frac{1}{2k}U$$

where

$$U(x_1, x_2, x_3, x_4) = V'(x_1^*, x_2^*, x_3^*, x_4^*) =$$
$$V'(x_1 + z_0, x_2, x_3 + \sqrt{mg/k}, x_4)$$

The system output is $Y = [1, 0, 0, 0]X = x_1$. For convenience, denote $f_1 = -\frac{k x_3^2}{m} - 2\sqrt{\frac{kg}{m}} x_3$,

$$f_2 = -\frac{R}{2k}\left((x_1 + z_0)x_4 + (x_3 + \sqrt{mg/k})x_2\right).$$

Even now, a control scheme is presented to stabilize the states of maglev system. Our control objective is to stabilize all states of (3) to zero, that is to design control input to maintain the air gap z at its nominal value.

Similar to linear system, the sliding mode control of nonlinear system consists two relatively independent parts: firstly confirm that the motion on the sliding surface is globally stable, and then design a sliding control-

ler which causes the trajectories of the system to reach the sliding surface in finite time.

Denote the error variables as

$$e_1 = x_1,$$
$$e_2 = x_2,$$
$$e_3 = f_1 = -\frac{kx_3^2}{m} - 2\sqrt{\frac{kg}{m}}x_3,$$
(4)
$$e_4 = \dot{f}_1 = -2(\frac{kx_3}{m} + \sqrt{\frac{kg}{m}})x_4.$$

Then a switching surface is defined as $s = c_1 e_1 + c_2 e_2 + c_3 e_3 + e_4$, where c_1, c_2, c_3 are selected to be positive constant numbers such that the polynomial $\lambda^3 + c_3 \lambda^2 + c_2 \lambda + c_1$ is Hurwitz. The error dynamics in sliding mode are thus asymptotically stable.

The second step is to design a sliding controller such that the sliding surface approaches 0. And the control input U can be formulated as

$$U = -[\frac{1}{2k}\frac{\partial f_1}{\partial f_3}]^{-1}\{c_1 x_2 + c_2 f_1 + c_3 \frac{\partial f_1}{\partial f_3}x_4 +$$
$$\frac{d}{dt}[\frac{\partial f_1}{\partial f_3}]x_4 + \frac{\partial f_1}{\partial f_3}x_2 + \beta sign(s)\}$$
(5)

where β is a positive constant.

Theorem 1. Under the control (5), all states of (4) will asymptotically converge to zero.

Proof. Select a Lyapunov function candidate: $V = s^2/2$. Differentiating V and substituting (4)-(5) yield,

$$\dot{V} = s\dot{s} = s[c_1\dot{e}_1 + c_2\dot{e}_2 + c_3\dot{e}_3 + \dot{e}_4]$$
$$= s[c_1 x_2 + c_2 f_1 + c_3 \frac{\partial f_1}{\partial f_3}x_4 + \frac{d}{dt}(\frac{\partial f_1}{\partial f_3})x_4 + \frac{\partial f_1}{\partial f_3}(f_2 + \frac{1}{2k}U)]$$
$$= -s \cdot \beta sign(s) = -\beta |s| \le 0$$
(6)

For the controller (5), inequality (6) implies that the system can reach the surface, $s = 0$, in finite time. β represents the amplitude of related to the sign-function, which has a relationship to the velocity of reaching the sliding surface. Since c_1, c_2, c_3 are selected to be positive constant numbers such that the polynomial $\lambda^3 + c_3 \lambda^2 + c_2 \lambda + c_1$ is Hurwitz, e_1, e_2 and e_3 will all converge to zero from any initial conditions. On the ideal sliding mode $s = 0$, that is $e_4 = -c_1 e_1 - c_2 e_2 - c_3 e_3$, e_4 will converge to zero too.

Then, we explain the vector $X = [x_1, x_2, x_3, x_4]^T$ will converge to 0 if $E \to 0$. From (4), we get that $e_1 = x_1, e_2 = x_2$ and $e_3 = f_1$ are stabilized. In practical

application, the current I and the air gap z are positive, so $x_3^*(=I/z)$ must be positive from Equation (2), then $x_3(=x_3^* - \sqrt{mg/k})$ should be larger than in Equation (3). It follows that x_3 has to converge to zero from the stability of $e_3 (= f_1 = -\frac{kx_3^2}{m} - 2\sqrt{\frac{kg}{m}}x_3)$. Similarly x_4 will converge to zero if e_4 is stabilized. Therefore, under the controller (5), the state variables of system (3) will all converge to the equilibrium point.

3. Adaptive Sliding Mode Controller Design

In order to eliminate the chattering typically found in conventional sliding mode control, we utilize the boundary layer technique [14,15,18]. If the control gain constant and the width of the boundary layer are fixed numbers, there is no guarantee for fast convergence. So we introduce an auto-tuning neuron to be the direct adaptive neural controller. The structure of an auto-tuning neuron can be mathematically expressed as [14,15,18]: $\sigma = E - \varphi$, where E represents the external input of neuron; φ denotes threshold of bias, and σ is the internal state of neuron.

The auto-tuning sliding mode control law for system (3) is

$$U = -[\frac{1}{2k}\frac{\partial f_1}{\partial f_3}]^{-1}[c_1 x_2 + c_2 f_1 + c_3 \frac{\partial f_1}{\partial f_3}x_4 + \frac{d}{dt}[\frac{\partial f_1}{\partial f_3}]x_4 + \frac{\partial f_1}{\partial f_3}f_2] + \phi(\sigma),$$
(7)

where $\phi(\sigma)$ is a modified hyperbolic tangent function,

$$\phi(\sigma) = \frac{a[1 - \exp(-b \cdot \sigma)]}{1 + \exp(-b \cdot \sigma)},$$
(8)

where a is the saturated level; and b is the slope value. Obviously, the shape of the nonlinear saturated function is governed by the values of both a and b. Figure 2 gives the plot of (8), where two adjustable parameters a and b influence mainly the output range and the curve shape of the activation function. A larger b corresponds to a narrower boundary layer. Let $\theta = [a, b, \varphi]^T$ represent the vector of adjustable parameters.

In the following we will adjust θ to achieve the control objective. The auto-tuning law is designed as

$$\dot{a} = -\eta e_1 sign(\frac{\partial x_1}{\partial U})(\frac{1 - \exp(-b \cdot \sigma)}{1 + \exp(-b \cdot \sigma)}),$$
$$\dot{b} = -\mu e_1 sign(\frac{\partial x_1}{\partial U})a\sigma,$$
(9)
$$\dot{\varphi} = -\dot{\sigma} = \gamma e_1 sign(\frac{\partial x_1}{\partial U})ab,$$

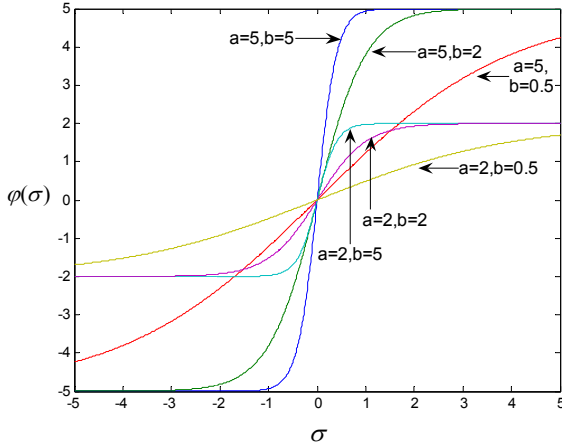where η, μ and γ are positive constants used to ad-

Figure 2. Modified activation function for different a and b.

just the convergence speed, and sign $\frac{\partial x_1}{\partial U}$ determines the direction of the search for θ. The accurate value of $\frac{\partial x_1}{\partial U}$ is not important since the maglev system output monotonically increases as the control input to the controlled plant increases, that is system (3) is said to be positive responded [18]. Then the system direction is written as 1. Fortunately, there are many industrial process control systems that possess the property of positive-responded or negative-responded.

Theorem 2. Under the control (7) and (8), all states of the system (3) with the adaptation law (9) will aymtocally converge to 0.

Proof. Consider the Lyapunov function candidate: $V = \frac{1}{2}e_1^2$. Differentiating V [14,15,18], we have

$$\frac{dV}{dt} = \frac{\partial V}{\partial e_1} \frac{\partial e_1}{\partial x_1} \frac{\partial x_1}{\partial U} (\frac{\partial U}{\partial a} \frac{\partial a}{\partial t} + \frac{\partial U}{\partial b} \frac{\partial b}{\partial t} + \frac{\partial U}{\partial \sigma} \frac{\partial \sigma}{\partial \varphi} \frac{\partial \varphi}{\partial t}) \quad (10)$$

For convenience, denote the first term of the right hand side of (10) $V_1 = \frac{\partial V}{\partial e_1} \frac{\partial e_1}{\partial x_1} \frac{\partial x_1}{\partial U} \frac{\partial U}{\partial a} \frac{\partial a}{\partial t}$, the second term and the third $V_2 = \frac{\partial V}{\partial e_1} \frac{\partial e_1}{\partial x_1} \frac{\partial x_1}{\partial U} \frac{\partial U}{\partial b} \frac{\partial b}{\partial t}$, $V_3 = \frac{\partial V}{\partial e_1} \frac{\partial e_1}{\partial x_1} \frac{\partial x_1}{\partial U} \frac{\partial U}{\partial \sigma} \frac{\partial \sigma}{\partial \varphi} \frac{\partial \varphi}{\partial t}$.

Substituting (7), (8) and (9) into (10) yield

$$V_1 = \frac{\partial V}{\partial e_1} \frac{\partial e_1}{\partial x_1} \frac{\partial x_1}{\partial U} \frac{\partial U}{\partial a} \frac{\partial a}{\partial t}$$

$$= e_1 \frac{\partial x_1}{\partial U} \frac{\partial}{\partial a} \{-[\frac{1}{2k} \frac{\partial f_1}{\partial x_3}]^{-1}[c_1 x_2 + c_2 f_1 + c_3 \frac{\partial f_1}{\partial x_3} x_4 +$$

$$\frac{d}{dt}(\frac{\partial f_1}{\partial x_3})x_4 + \frac{\partial f_1}{\partial x_3} f_2] + \frac{a[1-\exp(-b\cdot\sigma)]}{1+\exp(-b\cdot\sigma)}\}\dot{a}$$

$$= -\eta e_1^2 \left|\frac{\partial x_1}{\partial U}\right| (\frac{1-\exp(-b\cdot\sigma)}{1+\exp(-b\cdot\sigma)})^2 \leq 0$$

Similarly, V_2, V_3 become respectively:

$$V_2 = \frac{\partial V}{\partial e_1} \frac{\partial e_1}{\partial x_1} \frac{\partial x_1}{\partial U} \frac{\partial U}{\partial b} \frac{\partial b}{\partial t}$$

$$= -\mu e_1^2 \left|\frac{\partial x_1}{\partial U}\right| \frac{2\exp(-b\cdot\sigma)}{(1+\exp(-b\cdot\sigma))^2} a^2\sigma^2 \leq 0$$

$$V_3 = \frac{\partial V}{\partial e_1} \frac{\partial e_1}{\partial x_1} \frac{\partial x_1}{\partial U} \frac{\partial U}{\partial \sigma} \frac{\partial \sigma}{\partial \varphi} \frac{\partial \varphi}{\partial t}$$

$$= -\gamma e_1^2 \left|\frac{\partial x_1}{\partial U}\right| \frac{2\exp(-b\cdot\sigma)}{(1+\exp(-b\cdot\sigma))^2} a^2 b^2 \leq 0$$

where $e_1 \frac{\partial x_1}{\partial U}$ represents system output error contributed by the control input [18].

Since $\frac{\partial V}{\partial t} \leq 0$ while $V > 0$, according to the Lyapunov stability theory, V will decrease to zero, so $e_1 \to 0$, and $e_i (i = 2,3,4) = 0$. Therefore, similarly to the last paragraph in the proof of Theorem 1, the states of system (3) will all converge to zero.

4. Simulation and Results

In this section, we give the numerical simulation results of maglev system. The parameters and initial conditions used in the maglev system are given by $z_0 = 0.010m$, $m = 500kg$, $R = 4.4\Omega$, $k = 0.002$, $x(0) = (0.00458, 0, 1, 0)^T$. The parameters and initial conditions of the controller for simulation are $c_2 = 22.25$, $\eta, \mu, \gamma = 0.1$, $\beta = 0.1$, $\theta(0) = (-0.1, 0.2, 0)T$, and time interval is $t = 0.0001$,

As we know, the learning rate η, μ, γ play an important role in parameter learning process. For instance, a larger learning rate can accelerate the system response, but may also cause the system to have a larger overshoot. In the design of switching surface, $s = c_1 e_1 + c_2 e_2 + c_3 e_3 + e_4$, pole placement methodology [19] is often adopted to place the roots of the characteristic polynomial in desired region of the complex plane. That is, the control system denoted by the characteristic polynomial should have suitable damp, fast system response, short settling time and small overshoot. Therefore, c_1, c_2, c_3 are often chosen such that the three order polynomial has a pair of conjugate complex roots with negative real parts and a negative real root. When $c_1 = 21.75$, $c_2 = 22.25$, $c_3 = 8$, the roots of the characteristic polynomial are $-2.5 \pm 1i$ and -3.

Our control object is to design the control input to regulate the air gap to the desired value. Figure 3(a) and (b) represent the performance of state x_1 and the control input U by using the traditional sliding mode con-

ENGINEERING

trol, and it can be seen that the chattering around $x_1 = 0$ have occurred. The control input is regulated with high-frequency, which is not expected in industrial field. Figure 4(a) and (b) show the results by using our proposed method. Here, we choose $c_1 = 12$, $c_2 = 14$, $c_3 = 6$. The state x_1 is asymptotically controlled to 0 and the control input U is modulated. In Figure 4(a), the regulation time of state x_1 is about 6 second and the overshoot is near to 0.6 mm. In Figure 4(b), the overshoot of control input is reduced to 2. These verify that better control performance of maglev system can be achieved by the proposed auto-tuning controller.
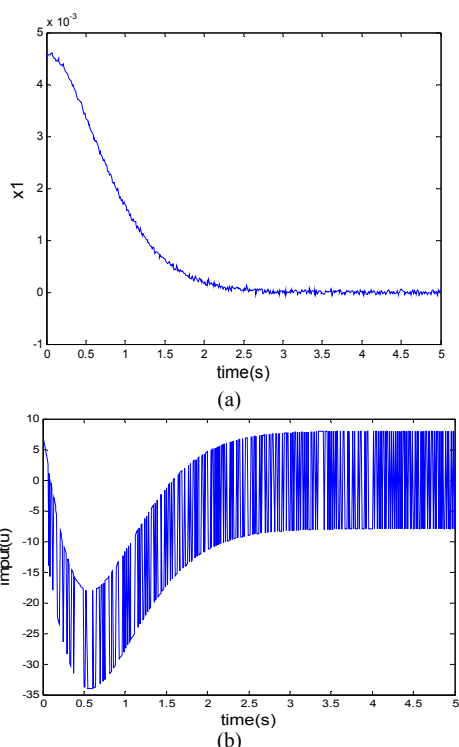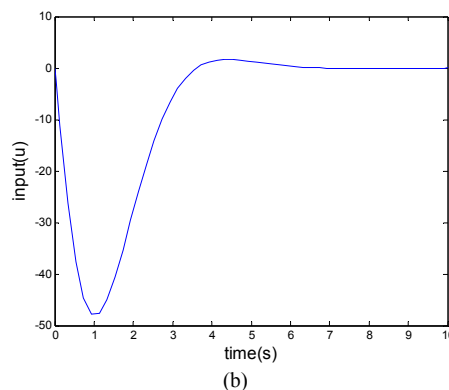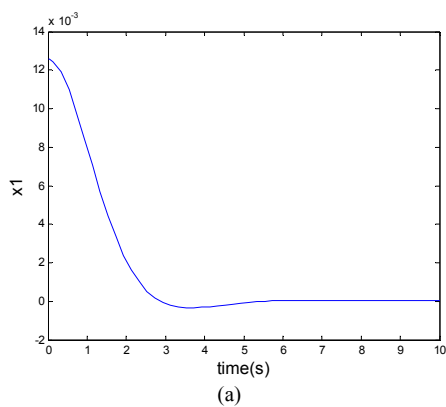

Figure 4. (a-b) show the results using the auto-tuning sliding mode control with control parameters $c_1 = 12$, $c_2 = 14$, $c_3 = 6$.

(a)

(b)

Figure3. (a-b) represent the control performance using the general sliding mode control.
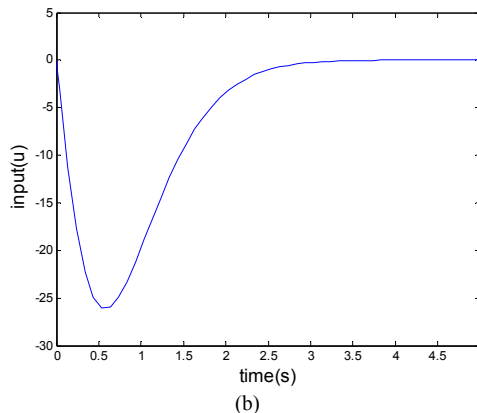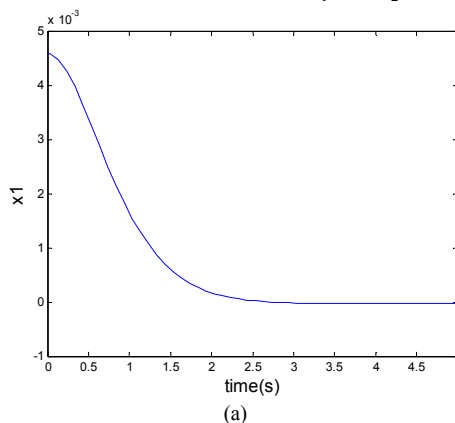

(a)

(a)

(b)

Figure 5. (a-b) show the results using the auto-tuning sliding mode control with control parameters $c_1 = 4$, $c_2 = 6$, $c_3 = 4$.

In Figure 4, the regulation time and overshoot is not satisfying, so here some new parameters $c_1 = 4$, $c_2 = 6$, $c_3 = 4$ by the proposed auto-tuning sliding mode control are chosen to accelerate system response and decrease the overshoot. In Figure 5(a), the convergence time of state x_1 slows to 3 second and the overshoot x_1 falls to 0. In Figure 5(b), the overshoot of control input is reduced to 0. It accords with the theoretical analysis. Based on the demand of practical application,

we can regulate these parameters to get a better performance.

5. Conclusions

In this paper, we discuss the problem of vibration control of maglev problem via a sliding mode control approach. In order to eliminate the high control activity and chattering caused by the general sliding mode control, we present an auto-tuning law based on the Lyapunov stability theory to guarantee the convergence of the system states. Simulation results verify the proposed auto-tuning controller is better than the traditional sliding mode controller.

It should be pointed out that only three control parameters are chosen to achieve good performance for maglev system in this paper, but other factors also can be applied to sliding mode control in practice. Next plan is to combine with more state variables with elastic guideway conditions. The expected results should improve the suspension performance of flexible guideway with proposed control algorithms.

6. References

[1] Y. Yoshihide, F. Masaaki, T. Masao, *et al*, "The first HSST maglev commercial train in Japan," MAGLEV 2004 Proceedings, pp. 76–85, 2004.

[2] R. Goodall, "Dynamic and control requirements for EMS maglev suspension," MAGLEV 2004 Proceedings, pp. 926–934, 2004.

[3] H. Wang, J. Li, K. Zhang, "Non-resonant response, bifurcation and oscillation suppression of a non-autonomous system with delayed position feedback control," Nonlinear Dynamic, Vol. 51, pp. 447–464, 2008.

[4] L. Zhang, L. Huang, Z. Zhang, "Stability and Hopf bifurcation of the maglev system with delayed position and speed feedback control," Nonlinear Dynamic, Vol. 57, pp. 197–207, 2009.

[5] C. Feng, W. U. Zhu, "Stochastic optimal control of strongly nonlinear systems under wide-band random excitation with actuator saturation," Acta Mechanica Solida Sinica, Vol. 21, No. 2, pp. 116–126, 2008.

[6] N. Taher, "A new fuzzy adaptive hybrid particle swarm optimization algorithm for non-linear, non-smooth and non-convexeconomic dispatch problem," Applied Energy,doi:10.1016/j.apenergy.2009.05.016, 2009.

[7] H. Tomohisa, M. Wassim, Y. Konstantin, "Neural network hybrid adaptive control for nonlinear uncertain impulsive dynamical systems," Nonlinear Analysis: Hybrid Systems, Vol. 2, pp. 862–874, 2008.

[8] V. Suplina, U. Shaked, "Robust H1 output-feedback control of systems with time-delay," Systems and Control Letters, Vol. 57, No. 3, pp. 193–199, 2008.

[9] B. Giorgio, F. Leonid, P. Alessandro, *et al*, "Modern sliding mode control theory," Berlin, Spinker, 2008.

[10] J. J. Slotine, W. Li, "Applied nonlinear control," Englewood Cliffs (NJ), Prentice-Hall, 1991.

[11] Y. J. Huang, T. C. Kuo, "Robust position control of DC servomechanism with output measurement noise," Electrical Engineering, Vol. 88, pp. 223–338, 2006.

[12] K. Furuta, "VSS type self-tuning control," IEEE Transactions on Industrial Electronics, 40, pp. 37–44, 1993.

[13] P. M. Lee, J. H. Oh, "Improvements on VSS type self-tuning control for a tracking controller," IEEE Transactions on Industrial Electronics, Vol. 45, pp. 319–325, 1998.

[14] C. T. Chen, W. D. Chang, "A feedforward neural network with function shape autotuning," Neural Networks, Vol. 9, No. 4, pp. 627–641, 1996.

[15] W. D. Chang, R. C. Hwang, J. G. Hsieh, "Application of an auto-tuning neuron to sliding mode control," IEEE Transactions on Systems, Man, and Cybernetics-Part C, Vol. 32, pp. 517–529, 2002.

[16] T. C. Kuo, J. H. Ying, S. H. Chang, "Sliding mode control with self-tuning law for uncertain nonlinear systems," ISA Transactions, Vol. 47, pp. 171–178, 2008.

[17] X. Rong, Ä. O. ÄUmit, "Sliding mode control of a class of underactuated systems," Automatica, Vol. 44, pp. 233–241, 2008.

[18] X. Cui, K. G. Shin, "Direct control and coordination using neural networks," IEEE Transactions on Systems, Man, and Cybernetics, Vol. 23, No. 3, pp. 686–697, 1993.

[19] C. D. Richard, H. B. Rober, "Modern control systems," Addison Wesley Longman, 1993.